Design of a Bioelectronics Hybrid System in Real Time and in Closed Loop

Guilherme Bontorin, André Garenne, Colin Lopez, Gwendal Le Masson, and Sylvie Renaud

***Abstract*—Hynets, for Hybrid (living-artificial) Networks, are an efficient and adaptable experimental support to explore the dynamics and the adaptation process of biological systems. We present in this paper an innovative platform performing a real-time closed-loop between a cultured network (e.g. neurons) and an artificial processing (e.g. software processing or a robotic interface). The system gathers bioware, hardware, and software components and ensures the closed-loop data processing in less than 50 µs. We describe also a methodology that may help to standardize the description of some experiments. This method is associated to a full custom Graphical User Interface. We detail here the system choices, components, and performances.**

***Index Terms*—Bioelectronics, Closed loop systems, Real-time data processing, Hybrid (living-artificial) networks, MEA (MultiElectrode Arrays), *in vitro* cell culturing.**

I. Introduction

BIOELECTRONICS is the discipline resulting from the convergence of biology and electronics. It includes the design and use of electronics for biology and medicine. Medicine is a strong driver for bioelectronics as illustrated by devices such as: neural stimulators [1], brain stimulators [2], cochlear implants [3], neuromuscular reanimation [4], brain-machine interface [5]. Other devices are under investigation by a very active research community: retinal prostheses [6], cognitive prostheses [7], and detection of insulin need [8].

We focus here on Hybrid Networks (Hynet). Hynets are real-time closed-loop hybrid systems that embody living and artificial elements. "Closed-loop" means that there is a two-way communication between those parts, and that each one receives controlling inputs from the other. "Real-time" means that this communication is fast enough to avoid any serious break on the data flow (losing or delaying).

Hynets are unique platforms for integrative biology investigations. Electronics circuitry in Hynets can emulate a functional neural network embodied inside a living network to form a unique hybrid network, as long as real-time communication is ensured between the artificial and the living parts. By controlling the circuitry configuration and parameters, researchers can study the functionality and activity patterns of the hybrid neural network as a whole, or characterize the living part. As detailed in the last section of the paper, our system is intended to be used for the study of plasticity in living neural networks, the influence of electromagnetic fields on the connectivity of neural networks and the characterization of electrical activity in electrogenic cells and islets in the pancreas.

In all bioelectronics systems, the developer has to define specifications related to both biological and electronics fields. Concerning biology, options are: *in vivo* or *in vitro* experiments, acute slice or dissociate cultures, and intracellular or extracellular interfaces. On the electronics point of view, rough implementation categories are: software or hardware, discrete components or integrated circuits (IC), and digital or analog data processing. Regarding the literature examples (Table I), we can see that almost all possible combinations of these choices, both in Electronics and Biology, are under investigation ([7, 9-18]).

Quantitative comparison of our system performances with the literature ([7, 9-18]) is however difficult: no standard exists to characterize it, and technical characteristics of experimental platforms are not always specified in publications. Our paper presents a precise and constrained evaluation of our system's design. It adds to [19], which was focused mostly on the hardware, a detailed description of the software and a template format to standardize the experiment description.

In this paper, we detail each choice and the consequent constituting blocks of our closed-loop in section II. Section III presents the detailed data flow, with the methodology we intend to promote standardization in experimental the description of experiments. Section IV describes time performances. This takes us to discuss the achievement and the uses of Hynet (section V).

II. Hynet Choices and Parts

The two parts, artificial and living, of the hybrid network (Hynet) communicate in bidirectional mode with each other: each provides outputs and receives controlling inputs from the other. The hardware and software parts of the artificial system run the bioware data acquisition, its processing, and the generation of feedback stimulation patterns. In this section, we

Manuscript received 10 June 2012. Received in revised form 16 December 2012. Accepted for publication 17 December 2012. This work was supported by the European Union, through the projects Neurobit (IST–2001-33564) and Facets (FP6-2004-IST-FETPI 15879).

G. Bontorin, C. Lopez and Sylvie Renaud are with the IMS Laboratory, University of Bordeaux, UMR 5218 CNRS, Bordeaux, France (e-mail: gbontorin@yahoo.fr). A. Garenne and G. Le Masson are with INSERM-E358, University of Bordeaux, 146 rue Léo Saignat, F-33076 Bordeaux, France.

DOI: 10.7251/ELS1216136B

TABLE I
EXAMPLES OF HYNETS AND THEIR BIOLOGICAL AND ELECTRONICS IMPLEMENTATION

Reference	First Author	Year	Cells	Interface	Feedback	Computing
[9]	Chapin	1999	*in vivo*	extracellular	visual	digital
[10]	Reger	2000	*in vitro*, acute	extracellular	discrete hardware	digital
[11]	Jung	2001	*in vitro*, acute	intracellular	integrated hardware	analog
[12]	Le Masson	2002	*in vitro*, dissociated	intracellular	integrated hardware	analog
[13]	Carmena	2003	*in vivo*	extracellular	visual	digital
[14]	Nowotny	2003	*in vitro*, dissociated	intracellular	software	digital
[15]	Oprisan	2004	*in vitro*, dissociated	intracellular	software	digital
[7]	Berger	2005	*in vitro*, acute	extracellular	integrated hardware	digital
[16]	Whittington	2005	*in vitro*, dissociated	extracellular	software	digital
[17]	Potter	2006	*in vitro*, dissociated	extracellular	software, discrete hardware	digital
[18]	Novelino	2007	*in vitro*, dissociated	extracellular	software	digital
-	This work		*in vitro*, dissociated	extracellular	software	digital

describe the three components of Hynet: the bioware, the hardware, and the software (Fig. 1).

A. Bioware

The first component of the system is the biological material that provides the signal for acquisition and is electrically stimulated. We develop our Hynet version to use it mostly in three experimental context: the study of plasticity in neural networks, the study of the influence of electromagnetic waves on neural networks, and the study of electrical activity of beta-cells of the pancreas as glucose sensors.

In the case of Hybrid Neural Networks [19], we use dissociated rat embryonic cortical cell cultures. Each MEA is plated with approximately 10^5 cells. After plating, the cells naturally tend to interconnect and create a complex neural network covering the MEA. The culture generally exhibits spontaneous spikes and bursts after 10-12 div (days-*in vitro*). In the case of insulin delivery control [8], we use cloned ß-cells from mice. They are cultivated for 6 div before the acquisition. The cells are routinely kept healthy and active for more than 3 months.

In all these cases, the study at the network level requires a multi-channels access to the culture, and long-term measurements. The common configuration for those experiments is: *in vitro* preparations of dissociated cells and extracellular multiple electrodes.

Extracellular electrodes, implemented on Multi Electrodes Arrays (MEAs) devices, are appropriate for the study of complex networks. They allow multisite acquisition and stimulation, without perforating the cell membrane. However, the biological signal, measured through capacitive coupling on the electrodes, is weak (~ 10-100 µV peak-to-peak to neurons), and the noise level (~ 1 mV at low frequencies) is high.

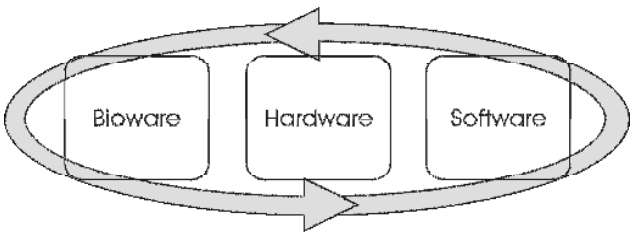

Fig. 1. The Hynet: The bidirectional communication path between the bioware and the software passes through the hardware.

Components of the biological signal can be separated as follows: (a) Extracellular Action Potentials (EAP); (b) Local Field Potentials (LFP); (c) Electrode-Electrolyte Interface Potential (EEIP); and (d) Stimuli Artifact (SA) [20-25].

EAP appear mostly in the frequency range from 0.1 kHz to 10 kHz. LFP are in the range from 1 Hz to 100 Hz. EAP and LFP come from the activity of the electrogenic cells [20]. EAP and LFP carry the meaningful activity information in the biological signal. EEIP comes from a near-to-DC potential difference between the solid electrode and the electrolyte solution. This potential varies spatially, from electrode to electrode, and temporally [21]. For example, with a gold recording site in buffered saline solution, this offset can be as high as ± 50 mV [22]. This is extremely large compared to EAP signal, usually in the range of 100 µV or LFP in the range of 1 mV [23].

SA depends from the external application of stimulation signals. Commonly used stimuli are in the range of the 1 V, which represents the largest signal range processed by the amplifier. After a stimulus, the EEIP takes milliseconds to evacuate the accumulated charge [24, 25].

EEIP and SA appear in low frequencies bands (< 0.1 Hz). They may hide the information (EAP and LFP).

Such an interface requires the use of carefully designed filters and amplifiers stages to process the biological signal. This is the importance of the Hardware.

B. Hardware

The second stage of the system is implemented on hardware, as a bridge between the bioware and the software. With the exception of the MCS (MultiChannel System™) suite (detailed later), all elements are custom made and assembled into a customized rack. This rack controls analog and digital signals, and it has an independent power supply and electrical references from those of the culture and of the computer. Hardware elements consist of a series of boards plugged into a modular and autonomous rack that conveys buses of shared data. All boards are configurable and work in real-time.

C. Software

The software is programmed in C++. It contains four basic parts, three of which are graphical user interfaces (GUIs) that

work offline and offer visual supports to control and monitor the experiment. The fourth one is the Real-time Application (ReTA) which recovers the information from the GUIs and from the hardware, and pilots the hardware. ReTA is the heart of the software part, and as such must be monitored to work in real time.

III. The Closed Loop

We detail in this section the tasks of the artificial part of the Hynet (Fig. 2). They are: A. the acquisition of biological data, B. the data processing resulting in decisions to close the loop, and C. the generation of electrical stimulation signals.

A. Acquisition

The hardware unit measures electrical signals from the cultures on the MEAs and conveys them to the software. Incoming analog signals have a low amplitude (10 ~ 100 µV, mainly in the 100-Hz – 10-kHz bandwidth) and a high noise level (up to 1 mV in lower frequencies and about 10 µVrms in the 100-Hz – 10-kHz band). The hardware outputs digital signals, with a 12-bit resolution and 40-kHz sampling frequency per acquisition channel. The hardware is composed of: the MCS suite, and boards identified as ACQ boards, DIGI boards and a PCI board (Fig. 2).

1) MCS suite: The bioware is plated on a multielectrode array, MEA200-30 from MultiChannel System™ (MCS) (diameter is 30 µm; interelectrode distance is 200 µm). The 60-electrode signals are available as parallel analog outputs of the MEA200-30. This MEA is inserted in the MEA1060 preamplifier from MCS, with a voltage gain of 1200. The preamplifier is connected to the BBMEA breakout box (for physical connections) from MCS. This system provides an easy access to the 60 recording analog channels [26].

2) ACQ board: we designed these boards to filter, isolate optically, and amplify the analog signals from bioware. Remaining EEIP noise is reduced by first-order high-pass filters (0.1 Hz cut-off frequency). The gain of each channel is individually controlled between 1 and 12 700. The gain's control signal uses a serial i2c protocol (Inter-Integrated Circuit [27]). Each ACQ board manages 4 channels, so for a complete 60-channel recording system, 15 ACQ boards are necessary. The amplified signals are conveyed to an analog bus in order to be digitalized.

3) DIGI board: this controls a subset of the rack's channels. More precisely, it manages:

3.a) the digitalization of the biological signals. The board is equipped with a Xilinx® FPGA (configurable digital circuit) that controls 2 Analog-to-Digital Converters (ADC). Each ADC converts each one of the 8 channels with a resolution of 12 bits and sampling frequency of 40 kHz. This sampling rate is specified to ensure a high quality reconstruction of the neurons dynamics for offline processing. Furthermore, as the A/D conversion is implemented within the rack, no analog signal is conveyed inside the digital environment of the computer, which limits the noise.

3.b) the data transfer between the rack boards and the computer PCI (Peripheral Component Interconnect) board. The acquisition data is transferred in parallel mode, as it may correspond to a large data flow if all channels are active; stimulation data, which is sparser, is transferred serially. Both are clocked at 16 MHz.

3.c) the control of the i2c bus, that manages the data, control and clock signals for the acquisition boards (ACQ) and for the stimulation boards (STIM and STT detailed further).

Each DIGI board controls 16 acquisition channels and 8 stimulation channels. For a 60-acquisition and 30-stimulation channels Hynet system, 4 boards are necessary.

4) PCI board: this board is the bridge between the rack and computer's PCI (Peripheral Component Interconnect) bus. The necessary data transfer rate for a 60-channel Hynet is approximately 5 MiB/s, (with 12 bits – 40 kHz sampling per channel), well below the 133 MiB/s (133.220 bytes per second) of the PCI transfer protocol. The PCI driver module is written in C++ and runs on Windows XP™. Other operating systems may provide a better platform for real-time processing with complex functions. However we chose to use Windows XP as our software performs real time in the experiments we conducted, and it is supports other proprietary software used during or after the experiments (MCS suite, Matlab). Currently, the software launches a warning/error sequence if 2 consecutive samples are not processed in real time.

The hardware we developed for the Hynet is not competitive with current commercial system [26, 28] in terms of static performances; but although individual boards process less

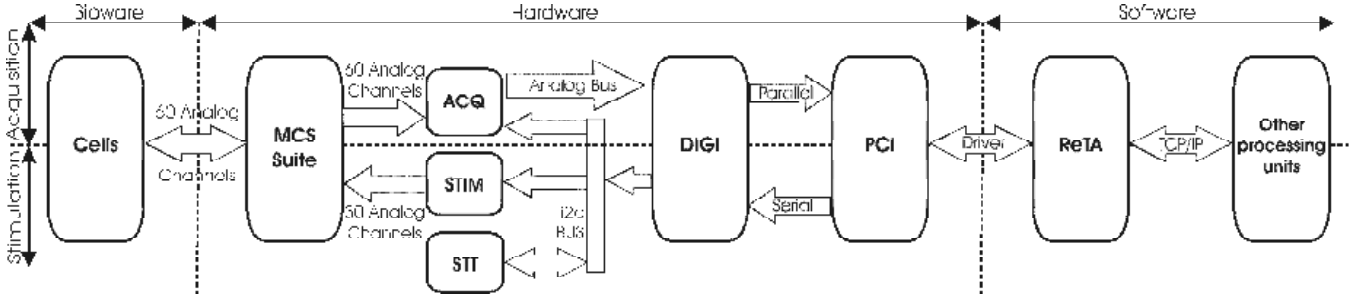

Fig. 2. Detailed view of the Hynet closed loop. The acquisition begins by the MultiChannel System™ (MCS) suite, with 60 analog channels. Signals are amplified by the ACQ boards and digitized by the DIGI board. The PCI board conveys the digital signals to the software domain. The Real-Time Application (ReTA) processes the data and can pass it to other processing units by a TCP/IP communication. The stimulation flow starts at the software level, initiated by an external processing unit or by the ReTA. The PCI board sends the control commands serially to the DIGI board. The Stimulation Trigger (STT) and Stimulation boards (STIM) convert the digital signals into 30 analog signals that are applied to the culture by the channels of the MCS Suite.

channels, the user can customize the experiment thanks to the modular architecture and the boards' configurability.

However the real benefit of the system lies in the real-time features of the processing (including the software) that are not present in commercial systems.

The biological signals are available to the software, which is designed as a Real-Time Application (ReTA). Its functions are:

1) Raw signal monitoring: data from 60 channels can be displayed in real time on the computer screen (Fig. 3.A). A zoomed view can also be selected for a single channel (Fig. 3.C).

2) Events detection: three types of patterns are extracted from the raw neural data: spikes, bursts, and stimulus artifacts.

A spike is a short electrical depolarization of a cell membrane. Extracellular spikes often reach amplitudes of 50 µVeil (equivalent input level). After hardware processing, noise amplitudes are estimated to be about 15 µVeil. Thanks to this level difference between spikes and noise, spikes can be detected by thresholding the signal, but the optimum threshold AC and DC may differ over the channels or even evolve over time.

ReTA presents two techniques to set the threshold. The first one is to define it as a fixed voltage value, defined by the user (for example by looking at the monitored signal). The second use the standard deviation (SD) of the signal as an estimation of the noise. The threshold is defined as a multiple (n) of SD. "n" is normally set in between 3 and 5, in order to avoid spike detection errors (false negative or false positive detection).

In order to present less than 1 ‰ of false positive decisions (the system interprets noise as a spike), "n" is usually set to be larger than 3. The maximum value is 5, after which the false negative decisions (true spikes are not detected) are too frequent. SD is continuously updated on line.

For our application, a "burst" is a pattern of N spikes on the same channel in a temporal window of duration W. For example, if a channel has three or more spikes (N = 3) in less than 10 ms (W = 10), this event is considered to be a burst. Both values, N and W, are programmable by the user before the experiment.

To implement burst detection, we create at the start of the experiment a circular buffer for each channel where a burst detection is required. Taking into account the sampling frequency (f) of the acquisition, the number of elements of a buffer is (W.f). After each acquisition sampling, the buffer is updated; depending on the values of the first element and the new element, the total number of spikes (S) is changed; the first element is overwritten by the new element; and the pointers of last and first elements are increased. If the total number of spikes in the buffer reaches the number of spikes in

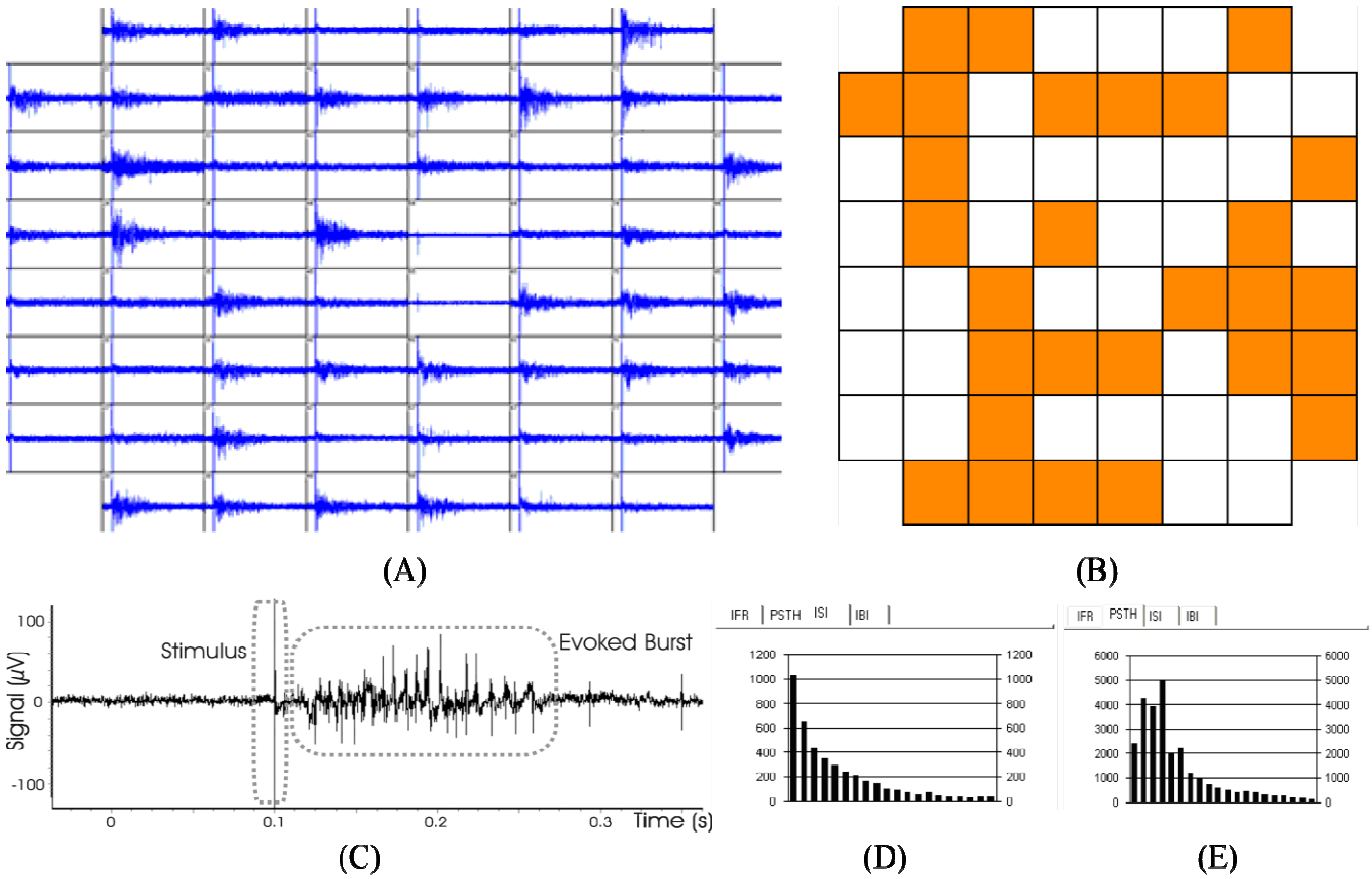

Fig. 3. Real-time monitoring of neural bursting activities induced by stimulations. (A) 60 raw signals in 1-second windows. (B) Bursts detection figure on the 60 channels; white: no burst detected; grey: burst detected within the last 0.25 s. (C) A zoomed view of one channel. We highlighted the stimulus and evoked burst. (D) Inter-Spike Interval (ISI) and (E) Post-Stimulus Timing Histogram (PSTH) for one channel. IFR stands for Instantaneous Firing Rates, IBI stands for Inter-Burst intervals; IFR and IBI are not presented here.

a burst ($S \geq N$), a burst is validated for the current timestamp.

Stimulus artifacts are detected by a simple thresholding method. Biologically effective stimulations generate artifacts that saturate the acquisition channel. Consequently, the threshold is relatively easy to fix before the experiment.

3) Events detection monitoring: The three types of events can be monitored online. The events evolution over time is indicated by color coding (Fig. 3.B). Inactivated channels are white. Once an event is detected, the corresponding channel passes immediately to red, and then progressively lightens: it provides visual information about signal propagation in the culture.

4) Statistics computing: the online detected events are also used to compute statistics, such as instantaneous firing rate (IFR), inter-burst interval histogram (IBI), inter-spike interval histogram (ISI), and post-stimulus-time histogram (PSTH). These statistics are commonly used in neurophysiology experiments. They are also plotted online (Fig. 3 D and E).

5) Storage: All the data are stored on the hard disk for offline analysis. The raw signal is stored in a 12-bit format, and a transtyping operation is done to save space disk. Events and Statistics are stored as timestamps in a text file.

6) Channels selection: To optimize the computational load, the user can configure processing on an individual channel. Useless channels can be deactivated, keeping more resources for ReTA or other real-time programs running on the same machine.

7) TCP/IP interface: In order to share the information with other programs, a TCP/IP (Transmission Control Protocol/Internet Protocol) interface is included in ReTA. The packages are configurable: they provide the timestamps and statistics of a selected event.

B. Closing the loop with the software

Our methodology to configure the closed-loop experiment comprises four software steps (Fig. 4.A):

1) The Condition Descriptor: configures the events in the acquisition that launch a stimulation pattern. A pattern can be launched: (a) continuously and/or periodically during all the experiment; (b) only at the beginning of the experiment (e.g. for a training or calibration task); (c) in response to a manual user request (e.g. by clicking a button); (d) in response to requests from another program, received through a TCP/IP interface; the purpose of this feature is to allow ReTA to interact with other programs; or (e) if a condition in the acquisition is reached. The condition in the acquisition can be defined as a complex input pattern. This pattern is defined by a sequence of time intervals (ΔT). Each interval has a quantity of spikes, bursts or statistics (N) and a test (equal, greater, lower). Fig. 4.C shows the window of our Condition Descriptor. Fig. 4.D shows a complex condition based on a spike detection. These patterns are stored in a file, which can be stored in a library.

2) The Pattern Descriptor: configures the stimulation patterns. The basic element of the pattern is the pulse. Bipolar voltage pulses, starting with the positive cycle, have been reported in the literature to be efficient (with respect to measurements of the responsiveness of neuronal cultures) and secure (considering the mean life time of neuronal cells) [24, 25]. Four parameters are tunable in a bipolar pulse: the positive (V+) and the negative (V-) voltage levels, and the positive (TV+) and the negative (TV-) widths. The pulse width varies from 50 µs to 3.27 s, with a 50 µs step, and the pulse levels range varies from 0 to ±10 V, with a 4 mV step. In a second level of abstraction, pulses can be repeated inside a "group". Two parameters are configurable in a group: the number of pulses and the pulse period. The last level of abstraction is the pattern, composed of the repetition of groups with a defined group period. Fig. 4.E presents GUI for the configuration of the stimuli pattern and Fig. 4.F the associated stimulation signal and its parameters. These patterns are stored in a file, which can also be stored in a library.

3) The Linker: defines the relationships between the conditions defined in step 1, the pattern described in step 2 and the stimulation channel. With this modular configuration, experiments can be designed with a reuse methodology, based on library elements (conditions, stimulation patterns from previous experiments). Logical AND, OR, and PIPE conditions, timers, and/or patterns are programmed at this stage. Fig. 4.G presents the GUI for the linker and Fig. 4.H shows an example of linking.

4) The Real-Time Application (ReTA): interprets the command files of the Linker, launches the different threads and circular FIFOs, establishes the TCP/IP communication, and drives the PCI (Peripheral Component Interconnect) card. Fig. 4.B presents the command window of the main GUI of the ReTA, effectively closing the loop of the experiment. In the center of the window, a panel displays the number of detected conditions (from step 1) or sent stimulations (from step 2) from and to the hardware.

C. Stimulation

After the Acquisition hardware and the Software, the Stimulation hardware completes the closed loop pathway.

The Stimulation hardware is the bridge back from the Software to the Bioware. The first blocks of the Stimulation hardware is the same PCI and DIGI boards as described for the acquisition. The DIGI board controls two types of boards used for stimulation: the Stimulation Trigger (STT) boards and Stimulation (STIM) boards (Fig. 2):

1) Stimulation Trigger (STT) Boards: these are in charge of triggering the stimulation signal (a biphasic stimulation pulse as described in the previous section). They provide individual trigger sequences for each channel. An i2c local bus controls this process. The resulting stimulation patterns can be configured by: the number of pulses in a group; number of groups in a pattern; periods of pulses and groups (Fig. 7.B), as configured in the step 2 of the software. Each STT board triggers 2 STIM boards, corresponding to 8 stimulation channels. A 32-channel stimulation setup requires 4 STT boards.

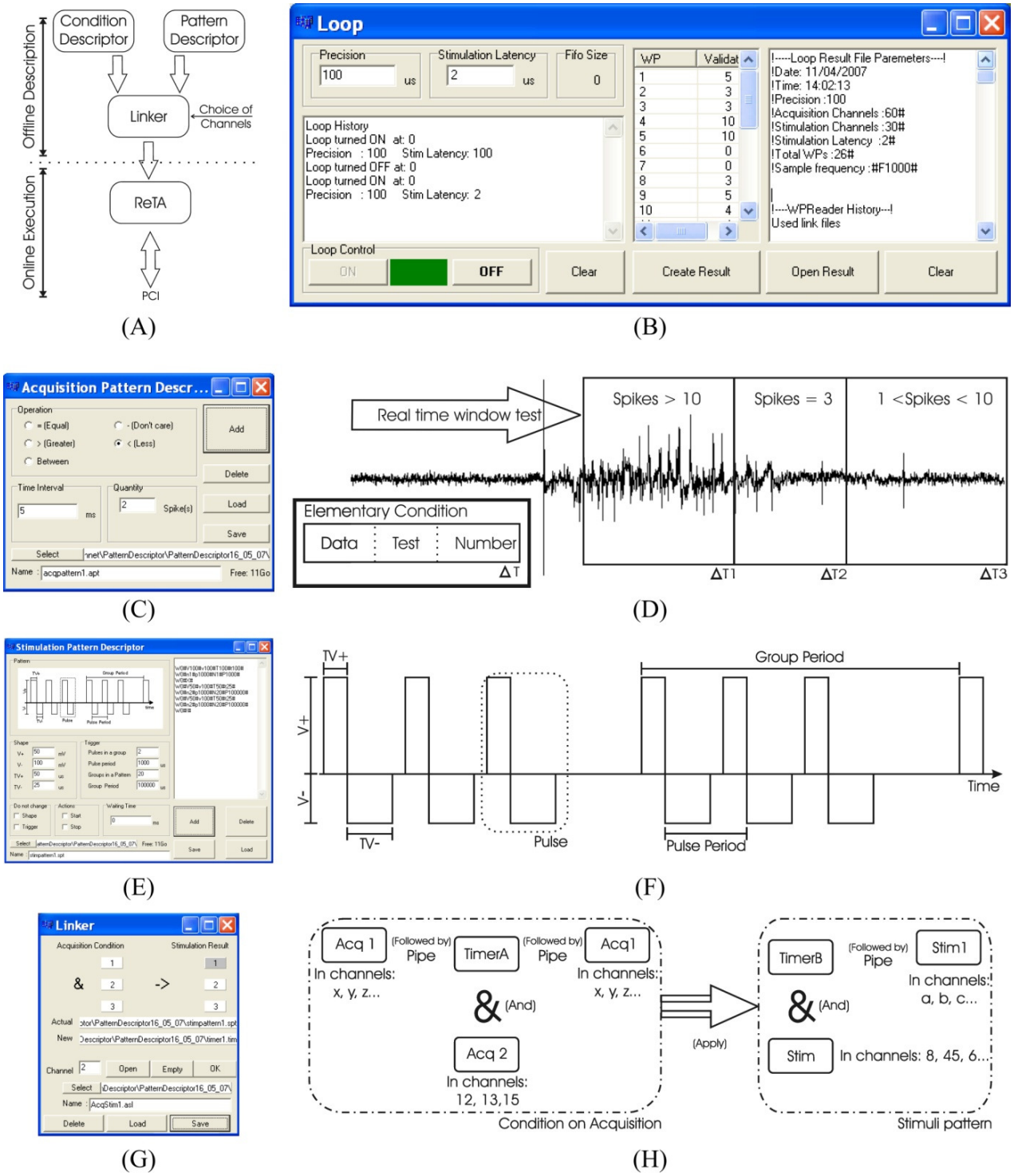

Fig. 4. Description of a closed-loop experiment. (A) The Condition Descriptor defines the acquisition pattern that triggers a stimulation. The Pattern Descriptor defines the stimulation signal. The Linker associates the relevant channels with the previous descriptions. The ReTA reads this configuration and processes online the data to and from the PCI. (B) The command window of the ReTA application closing the loop. The left part of the window presents the current status of the loop and its parameters. In the center box, the number of conditions detected or stimulations launched are updated in real time. This interface generates and reads reports of the experiments (right part of the window). (C) The Condition Descriptor's GUI window and (D) An example of condition setting. Three information compose one elementary condition: the data we are looking for (spike or statistics), the logical test (equal, less, greater, …), and the time interval ΔT. Each complex condition is composed of one or more basic conditions. In this example, the complex condition is composed of 3 elementary conditions. The first is the detection of more than 10 spikes over ΔT1; the second is the detection of exactly 3 spikes over ΔT2, and the last is the detection of at least 1 and less than 10 spikes over ΔT3. During the acquisition, a theoretical window sweeps the signal to look for the condition. (E) The Stimulation Pattern Descriptor's GUI window and (F) Example of a stimulation pattern and its parameters. Four parameters are tunable in a bipolar pulse: the positive (V+) and the negative (V-) voltage levels, the positive (TV+) and the negative (TV-) time widths. Two parameters are configurable in a group: the number of pulses and the pulse period. The last level of abstraction is the pattern, composed of the repetition of groups with a defined group period. (G) The Linker's GUI window. (H) An example of linking. The library elements from the previous steps (conditions, stimulation patterns and timers) are linked using logical functions AND, OR, PIPE conditions and the channels numbers. The Linker also relates the acquisition patterns (left part of the figure) to the stimulation patterns (right part of the figure).

2) Stimulation (STIM) Boards: these generate analog stimulation signals, which are applied to the MEA electrodes. Each board individually controls 4 stimulation channels. For a 32-channel stimulation system, 8 boards are necessary. Individual cables for each channel convey signals to the MCS suite.

The MCS suite is the same suite as the one used by the acquisition flow. The MEA has a parallel access for the acquisition and the stimulation of each of the electrode sites. The user configures the distribution of the stimulation channels among the 60 electrodes by on-board hardware switches.

We intentionally limited the number of stimulation channels to 30, as single stimulations are proven to already have an effect on a population of neurons distributed covering more than one channel. In any case, the number of stimulation channels could easily be increased on our system by adding more DIGI, STT, and STIM boards.

IV. Results

A. Acquisition

In extracellular measurements, as is the case of MEAs, the typical data bandwidth is about 3 kHz for spike detection [29], which implies a Shannon frequency of 6 kHz [30]. We chose to run our system with a minimum 10 kHz sampling rate (and then a period of 100 µs), to ensure a correct reconstruction of biological signals in real time. A higher sampling rate (e.g. 40 kHz) would give more information about spike shapes, which is not a priority for the experiments we plan.

Thanks to its tunable architecture, our acquisition system can provide different outputs changing its processing delay. We present the delays related to different experiments (A to E in Fig. 5), going from 25 µs (A) to 60 µs (E).

The simplest experiment (A) consists of an offline analysis. In this case, only the raw data storage and monitoring must be in real time. The mean delay is 25 µs (A). In this case the sampling frequency can be tuned to 40 kHz, increasing detail in the spike waveform.

Adding other real-time processes increases the delay. The most resource demanding online detection (event detection on all channels in a 10 ms burst window) adds 15 µs (B). One statistic function requires 15 µs (C).

The delay to send data to the TCP/IP layer is 5 µs on average. Raw data is not sent because it is too resource demanding. If event detections (D) and statistics (E) are sent, the process delays are, respectively, 45 µs and 60 µs.

In the most complex experiment, all the information (event and statistic) is sent to the TCP/IP layer with a mean delay of 60 µs. If we stick to the initial specification, for real time, of a 100 µs global delay, 40 µs are still available for user-defined additional functions.

B. Stimulation

Stimuli can originate from three different sources: (a) offline data programmed before the beginning of the experiment; (b) user action; and (c) requests from another program received by the TCP/IP interface. In terms of timing, (a) and (b) are directly implemented from the ReTA. For (c) we must take into account the time necessary for ReTA to access the data from the TCP/IP layer. Once the ReTA "knows" that it must launch a pattern, the mean time for processing through the PCI driver is about 5 µs. With 1 µs more, the data pass the PCI bus and access the DIGI boards. These delays suppose a PC with only ReTA running besides the Operating System (OS): the PCI bus must be permanently available for the Hynet. In any case, these delays are controlled and all buffers are monitored

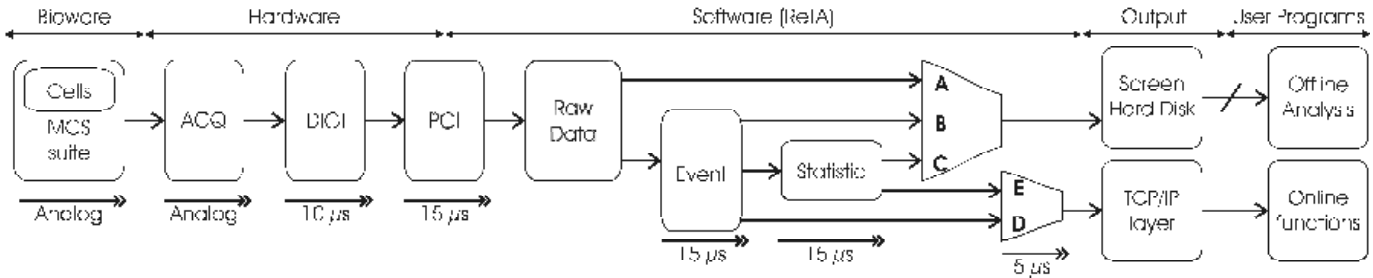

Fig. 5. Data propagation delays of the acquisition chain as described in Fig. 2 for different experimental configurations (A to E). The simplest experiment's delay is 25 µs for real-time raw data storage and monitoring (A). The most complex analysis requires 60 µs (E).

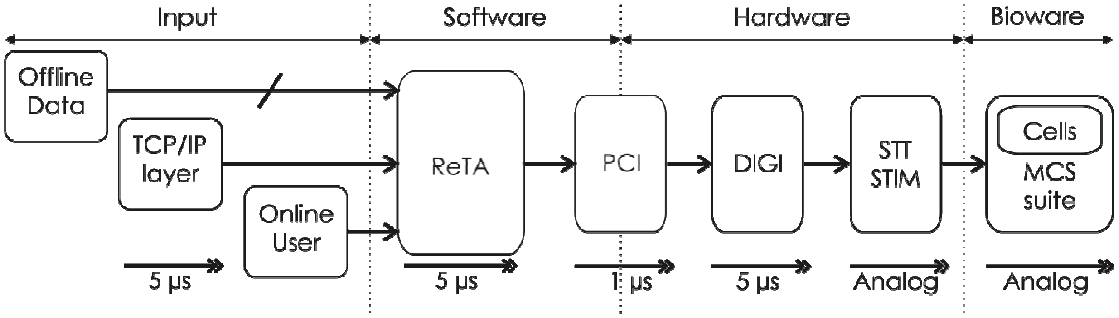

Fig. 6. Propagation delays for the stimulation chain (as described Fig 3). The total mean delay, from the command in the TCP/IP layer to the biological cells, is 16 µs.

(software access to internal registers and timings). If the delay for a task is too long, a warning/error sequence is launched.

From DIGI boards to STIM and STT boards, the programming time is 5 µs (fixed delay). Analog signals are transferred from the STIM boards to the cultures, with propagation delays that are negligible when compared to digital ones. The total delay for the stimulation chain is therefore 16 µs on average (Fig. 6).

C. Closed Loop

"Real time" in a Hynet system is a strict constraint: it implies that within the time step between 2 acquisitions, all the online processing on the available data has been executed (and has generated a consequent stimulation). The "closed-loop period" is the time taken by the system between the acquisition and the related feedback stimulation. This period should not bypass the maximum sampling period.

The propagation times across the modules of Hynet are summarized in Fig. 7. The software environment is Windows XP™ running on a Bi-Xeon, 4 GB RAM, 3 GHz PC. Measurements were made individually for each block.

A 10-kHz sampling frequency corresponds to a 100 µs period available for the loop. By summing the digital modules' delays (as the analog ones are negligible), we obtain a closed-loop period of 46 µs. In this case, we have the simplest acquisition chain (25 µs), a closing-loop sequence (5 µs), and the simplest stimulation chain (16 µs). More than 50 µs are then available for the software at each time step, to close the loop.

V. Discussion

Into this time interval of 50 µs, the ReTA can process a complex experiment as described in section III.B (Closing the loop with the software). The processing time for the closing loop depends on the complexity of the task. For example, we have applied on all 60 channels a condition composed of two terms. The first one is a spike firing rate between 2 and 10 in a time interval of 20 ms; the second term is a resting time (no spikes) during the following 20 ms. If the condition is fulfilled by any of the 60 channels, the system triggers a stimulus in all of the 30 stimulation channels. The average computation time for this test is 26 µs.

This Hynet system conveys fewer channels than current commercially available systems from MCS or BioLogic Science instruments [26, 28]. Its great advantage is the real-time closed loop. This feature is until now only present in research laboratories, with an equivalent number of acquisition, and similar (double) stimulation channels [17, 18]. The Hynet carries out a bidirectional communication between a cell culture and an artificial system. Communication in the Hynet is possible through multiple parallel channels, using the multielectrode interface. The transmission delay in the closed loop is low enough to allow a 10-kHz sampling rate and still leave time for processing reaction stimuli, whilst ensuring real-time. The Graphical User Interface (GUI) provides a friendly and portable interface; it proposes a template format to standardize the experiment description.

The Hynet system design is intended to be highly tunable. Different types of experiments are currently being conducted using the Hynet: we are investigating plasticity mechanisms in cortical neural networks [19], we are studying cultured neural networks exposed to electromagnetic waves, and we are exploring the dependence to glucose of the electrical activity of pancreatic beta-cells [8].

In studies on plasticity in neural networks, the role of the artificial part is to evaluate the relationship between the evolution of the network dynamics and a "consistent" feedback. By consistent feedback, we mean that the biological network is informed in real-time about the actual sensory consequences of its activity, just like an "unprogrammed" living organism embedded into the real world. In this "brain-in-a-box" paradigm, the biological brain is in communication with the "outside body". Two essential features are necessary for the experimental set-up in this project: (i) real-time biological signal processing and real-time communication (already functional in Hynet); and (ii) feedback functions to drive a dissociated network to adapt its evoked responses to stimuli in a learning-like process. Thus, we can use the Hynet to invest bioinspired learning and plasticity functions at the network and at the cellular level.

The second series of experiments using the Hynet system aims to study the influence of electromagnetic fields on neural networks. Cultured cortical preparations are exposed to repetitive and controlled fields (using a custom exposition system in which an MEA is embedded) that reproduce Bluetooth or other GSM microwaves. For such an experiment, the artificial part (presently computed by software) is a network of conductance-based neurons. The Hynet helps us to

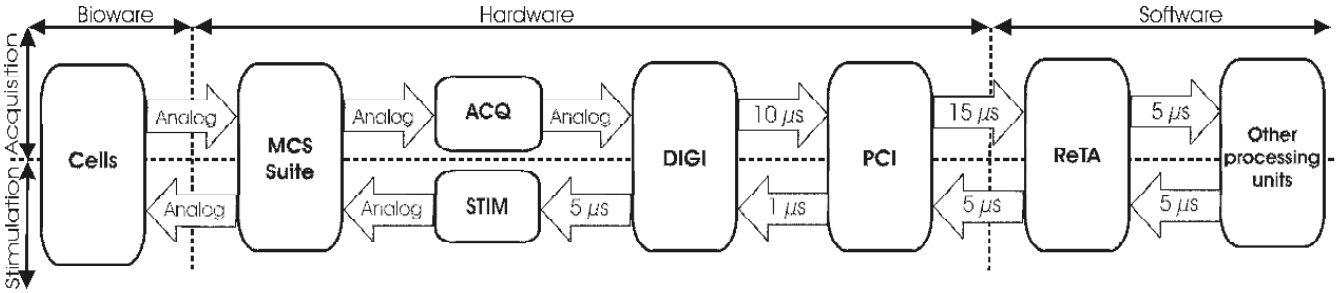

Fig. 7. Data propagation delays of the complete Hynet closed-loop. The minimum closed-loop processing period is 46 µs. For our specification (10 kHz sampling frequency), more than 50 µs are then available for the software during each period to close the loop.

investigate the evolution of activity and connectivity of biological cells, while the artificial neural network has inhibitory or excitatory actions to control or cancel this evolution. It may also be useful for investigating therapeutic usage of electromagnetic waves, although this is not its primary goal.

The third series of experiments, a study of electrical activity of beta-cells of the pancreas, could be useful in providing give a key to a better life for diabetics. The fundamental study on the behavior of such cells shows that the firing rate represents the glucose concentration and is modulated by agents such as the GLP–1 (Glucagon-like Peptide-1). This new model will help us to develop our understanding of the electrical code used by these cells to translate glucose/nutrient/hormone signals into precisely adapted secretion of insulin. A glucose sensor that reacts in real time, which is capable of taking hormones and other nutrients into account and of detecting hypo/hyperglycemia, represents an important need and challenge for life expectancy, life quality and medical costs of a growing number of diabetic.

Even though this system is operational and useful, it is of great interest to increase the number and the density of acquisition channels in order to increase the details of the information or simply for parallel computing performances. To increase the number of acquisition channels, we plan to integrate the preamplifier function, which is one of the factors that limit large-scale acquisition. Also, we intend to maintain the closed-loop real-time feature essentially for experiments that address the investigation of hybrid networks. Thus we intend to integrate data processing on the hardware part, with smart sensors.

REFERENCES

[1] F. Nsanze, "ICT Implants in the Human Body - A Review," The European Group on Ethics in Science and New Technologies to the European Commission2005.

[2] J. C. Robert, "Deep Brain Stimulation Devices: A Brief Technical History and Review," Artificial Organs, vol. 33, pp. 208-220, 2009.

[3] G. E. Loeb, "Cochlear Prosthetics," Annual Review of Neuroscience, vol. 13, pp. 357-371, 11/28/ 2003.

[4] G. E. Loeb, R. A. Peck, W. H. Moore, and K. Hood, "BION(TM) system for distributed neural prosthetic interfaces," Medical Engineering & Physics, vol. 23, pp. 9-18, 2001.

[5] M. A. L. Nicolelis and M. A. Lebedev, "Principles of neural ensemble physiology underlying the operation of brain-machine interfaces," Nat Rev Neurosci, vol. 10, pp. 530-540, 2009.

[6] J. D. Weiland and M. S. Humayun, "A biomimetic retinal stimulating array," Engineering in Medicine and Biology Magazine, IEEE, vol. 24, pp. 14-21, 2005.

[7] T. W. Berger, A. Ahuja, S. H. Courellis, S. A. Deadwyler, G. Erinjippurath, G. A. Gerhardt, et al., "Restoring lost cognitive function," Engineering in Medicine and Biology Magazine, IEEE, vol. 24, pp. 30-44, 2005.

[8] M. Raoux, G. Bontorin, Y. Bornat, J. Lang, and S. Renaud, "Bioelectronic sensing of insulin demand," in Biohybrid Systems, R. Jung, Ed., ed: Wiley-VCH, 2011.

[9] J. K. Chapin, K. A. Moxon, R. S. Markowitz, and M. A. L. Nicolelis, "Real-time control of a robot arm using simultaneously recorded neurons in the motor cortex," Nature Neuroscience, vol. 2, pp. 664 - 670, 1999.

[10] B. D. Reger, K. M. Fleming, V. Sanguineti, S. Alford, and F. A. Mussa-Ivaldi, "Connecting Brains to Robots: The Development of a Hybrid System for the Study of Learning in Neural Tissues," in Proc. of the VIIth Intl. Conf. on Artificial Life, 2000, pp. 263-272.

[11] R. Jung, E. J. Brauer, and J. J. Abbas, "Real-time interaction between a neuromorphic electronic circuit and the spinal cord," Neural Systems and Rehabilitation Engineering, IEEE Transactions on, vol. 9, pp. 319-326, 2001.

[12] G. L. Masson, S. Renaud, D. Debay, and T. Bal, "Feedback inhibition controls spike transfer in hybrid thalamic circuits," Nature, vol. 417, pp. 854-858, 2002.

[13] J. M. Carmena, M. A. Lebedev, R. E. Crist, J. E. O'Doherty, D. M. Santucci, D. F. Dimitrov, et al., "Learning to Control a Brain-Machine Interface for Reaching and Grasping by Primates," PLoS Biol, vol. 1, p. e42, 10/13 2003.

[14] T. Nowotny, V. P. Zhigulin, A. I. Selverston, H. D. I. Abarbanel, and M. I. Rabinovich, "Enhancement of Synchronization in a Hybrid Neural Circuit by Spike-Timing Dependent Plasticity," J. Neurosci., vol. 23, pp. 9776-9785, October 29, 2003 2003.

[15] S. A. Oprisan, A. A. Prinz, and C. C. Canavier, "Phase Resetting and Phase Locking in Hybrid Circuits of One Model and One Biological Neuron," Biophysical Journal, vol. 87, pp. 2283-2298, 2004.

[16] R. H. Whittington, L. Giovangrandi, and G. T. A. Kovacs, "A closed-loop electrical stimulation system for cardiac cell cultures," Biomedical Engineering, IEEE Transactions on, vol. 52, pp. 1261-1270, 2005.

[17] S. Potter, D. Wagenaar, and T. DeMarse, "Closing the Loop: Stimulation Feedback Systems for Embodied MEA Cultures," in Advances in Network Electrophysiology, ed, 2006, pp. 215-242.

[18] A. Novellino, P. D. Angelo, L. Cozzi, M. Chiappalone, V. Sanguineti, and S. Martinoia, "Connecting neurons to a mobile robot: an *in vitro* bidirectional neural interface," Intell. Neuroscience, vol. 2007, pp. 2-2, 2007.

[19] G. Bontorin, S. Renaud, A. Garenne, L. Alvado, G. Le Masson, and J. Tomas, "A Real-Time Closed-Loop Setup for Hybrid Neural Networks," in Engineering in Medicine and Biology Society, 2007. EMBS 2007. 29th Annual International Conference of the IEEE, 2007, pp. 3004-3007.

[20] R. R. Harrison, "The Design of Integrated Circuits to Observe Brain Activity," Proceedings of the IEEE, vol. 96, pp. 1203-1216, 2008.

[21] D. A. Robinson, "The electrical properties of metal microelectrodes," Proceedings of the IEEE, vol. 56, pp. 1065-1071, 1968.

[22] K. D. Wise and J. B. Angell, "A Low-Capacitance Multielectrode Probe for Use in Extracellular Neurophysiology," Biomedical Engineering, IEEE Transactions on, vol. BME-22, pp. 212-219, 1975.

[23] R. R. Harrison, "A Versatile Integrated Circuit for the Acquisition of Biopotentials," in Custom Integrated Circuits Conference, 2007. CICC '07. IEEE, 2007, pp. 115-122.

[24] D. R. Merrill, M. Bikson, and J. G. R. Jefferys, "Electrical stimulation of excitable tissue: design of efficacious and safe protocols," Journal of Neuroscience Methods, vol. 141, pp. 171-198, 2005.

[25] D. A. Wagenaar, J. Pine, and S. M. Potter, "Effective parameters for stimulation of dissociated cultures using multi-electrode arrays," Journal of Neuroscience Methods, vol. 138, pp. 27-37, 2004.

[26] MEA System User Manual, "MEA System User Manual," MultiChannel Systems, Ed., ed. Reutlingen, Germany, 2006.

[27] J.-M. Irazabal and S. Blozis, "Application note AN10216-0: I2C Manual," ed: Philips Semiconductors Inc., March 2003.

[28] BioMEA ref., "BioMEA," B. S. Instruments, Ed., ed. Claix, France, 2009.

[29] D. A. Henze, Z. Borhegyi, J. Csicsvari, A. Mamiya, K. D. Harris, and G. Buzsaki, "Intracellular Features Predicted by Extracellular Recordings in the Hippocampus In Vivo," Journal of Neurophysiology, vol. 84, pp. 390-400, 7/1 2000.

[30] C. E. Shannon, "Communication in the Presence of Noise," Proceedings of the IRE, vol. 37, pp. 10-21, 1949.